Optical Doppler tomography for monitoring vascularization during photodynamic therapy of skin cancer lesions

Thomsen, J; Bendsöe, Niels; Svanberg, Katarina; Andersson-Engels, Stefan; Jorgensen, T. M; Thrane, L; Larsen, H. E; Pedersen, F; Andersen, P. E

Published in:
BIOPHOTONICS: PHOTONIC SOLUTIONS FOR BETTER HEALTH CARE

DOI:
10.1117/12.781142

2008

Optical Doppler tomography for monitoring vascularization during photodynamic therapy of skin cancer lesions

J. Thomsen[a], N. Bendsøe[b], K. Svanberg[c], S. Andersson-Engels[d], T. M. Jørgensen[a], L. Thrane[a], H. E. Larsen[a], F. Pedersen[a], P. E. Andersen[a]

a. DTU Fotonik, Technical University of Denmark, Denmark
b. Department of Dermatology, Lund University Hospital, Lund, Sweden
c. Department of Oncology, Lund University Hospital, Lund, Sweden
d. Department of Physics, Lund University, Lund, Sweden

ABSTRACT

We investigate vascular changes during Photodynamic therapy (PDT) of skin tumors using optical Doppler tomography (ODT). The effect of vascular shut down on tumor destruction is currently not known, and to optimize treatment it is relevant to investigate this issue further. Optical Doppler tomography is capable of measuring blood flow in biological tissue down to 1-2 mm with sub-mm/s velocity sensitivity and micrometer spatial resolution making it suitable for blood flow measurements in the skin. We demonstrate the ability of detecting blood flow in the human skin using non-interstitial ODT to preserve the non-invasiveness. In general a very limited blood flow activity was observed in normal skin and around skin tumors making monitoring of changes difficult. We suggest solutions to a number of practical issues such as sampling errors and natural fluctuations in flow activity for future work.

Keywords: Photodynamic therapy, optical Doppler tomography, skin tumors, optical coherence tomography, blood flow

1. MOTIVATION

Photodynamic therapy (PDT) is a non-invasive well-established treatment of skin tumors with direct or more indirect effects leading to cancer cell death [1]. A sensitizer is absorbed in the tumor. Following an illumination of the tumor area with adequate wavelength, a photo-chemical process is induced and results in tumor destruction. The treatment effect can be divided in several categories – direct cell kill, indirect response due to vascular effects, and immunological responses. The importance of the vascular effect depends on several parameters such as the type of photosensitizer, its distribution pathway, and time between drug supply and light illumination. Understanding these processes in more detail is relevant to optimize the treatment. If the primary effect of PDT is a vascular damage, the time between sensitizer supply and light illumination should be chosen for maximal sensitizer concentration in the blood vessels. On the other hand, if the primary effect is tumor cell destruction, a maximal sensitizer concentration at critical locations in the tumor itself should be the goal. Monitoring blood flow during PDT may give a more detailed insight to the process of tumor destruction. Furthermore, blood flow measurements during PDT treatment may be used as a tool for deciding when to finish the treatment as well as a tool for the follow-up of treatments.

Laser Doppler perfusion imaging has previously been used for blood flow imaging, but does not provide spatial depth resolution [2]. By instead using optical Doppler tomography (ODT), information about spatial localization of blood flow is possible, and therefore adds additional knowledge. Monitoring vascular changes during PDT with ODT has previously been performed on animals during PDT using an interstitial implementation [3]. Here, we aim for in vivo blood flow measurements on human skin tumors during PDT. To preserve the non-invasiveness of OCT, we do not use an interstitial implementation.

2. OPTICAL DOPPLER TOMOGRAPHY SYSTEM

The OCT system used in this study is a mobile time domain system operating at 1300 nm. A sketch of the system is shown in Figure 1. The light source is a superluminescent diode with a power of 20 mW (ex fiber), and a bandwidth of 66 nm (FWHM) corresponding to a depth resolution of ~8 μm in tissue. The transverse resolution is determined by the

Biophotonics: Photonic Solutions for Better Health Care, edited by
Jürgen Popp, Wolfgang Drexler, Valery V. Tuchin, Dennis L. Matthews,
Proc. of SPIE Vol. 6991, 699118, (2008) · 1605-7422/08/$18 · doi: 10.1117/12.781142

spot size of the beam and is approximately 30 μm. Light from the source is coupled via a circulator into a fiber-based Michelson interferometer with a 50/50 beam splitter. The circulator is used to accomplish balanced detection to suppress excess noise from the light source thereby improving the signal-to-noise ratio. In the reference arm, we use an optical delay line employing a resonance scanner with a resonance frequency of 4 kHz equal to the A-scan rate [4]. In the Doppler mode, an electro-optical modulator (EOM) sets the carrier frequency of the interferogram to 3.2 MHz [5]. A lateral scan is provided by a galvanometer pivoting a mirror to obtain a B-scan image. Envelope and phase information are calculated in a FPGA board (Altera Corp. EP1S80) as recently implemented in another system [6]. The calculation of the envelope and Doppler frequency are described in more details below. When acquiring only structural OCT images, data is acquired using an analog frame grabber, and the EOM is switched off with the carrier frequency set by the delay line [4]. In Doppler mode, data is acquired using an USB interface, and the carrier frequency is then set by the EOM. The extraction of the phase shift between two following interferograms is made by the sequential scan processing algorithm [7]. The phase shift due to block motion of the probe or sample is reduced by a motion artefact rejection algorithm [8]. The sequential scan processing algorithm ensures high velocity sensitivity, and the motion artefact rejection makes it possible to visualize blood flow in vivo with a suppression of noise induced by inter probe-skin movements. By overlaying the flow information to the structural OCT image, so-called Colour Doppler OCT images are constructed.

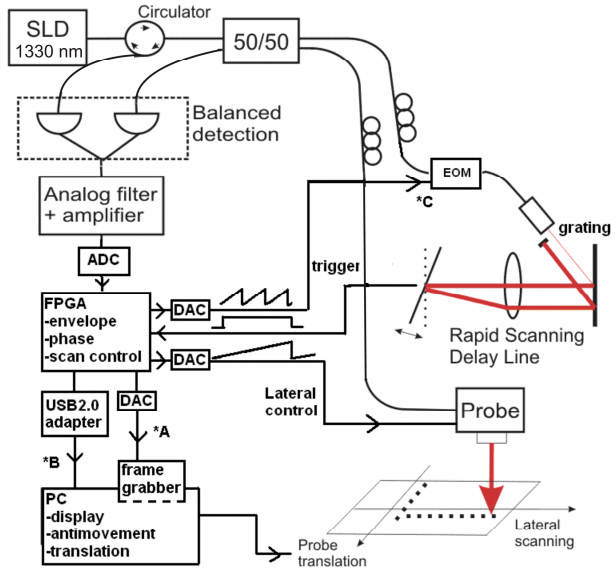

Figure 1. OCT system block diagram. When acquiring only structural OCT images, data is acquired using the analog frame grabber (*A), the EOM is switched off (*C), and the carrier frequency is set by the delay line. In Doppler mode, data is acquired using the USB interface (*B), and the carrier frequency is then set by the EOM.

In Figure 2 is a detailed block diagram of the signal processing performed with the FPGA. The amplified interferogram is digitized at a sample rate of 120 MS/s, and subsequently decimated by a factor 8 inside the FPGA. Decimation lowers the quantization noise and the effective number of bits. Additionally, the over-sampling relaxes the requirements on the analog anti-aliasing filter. The decimated signal is converted to an analytic signal by passing it through a digital filter, which eliminates the negative frequency components. Its envelope is calculated as the modulus of the analytic signal, and the phase as its argument. At each lateral location a number of 2 to 8 sequential scans are done. The resulting envelope at any given depth is calculated as the average of these values. The average phase change from one scan to the next is calculated using the Kasai autocorrelation [9]. This algorithm has the property that measurements with large amplitude have a higher contribution to the result as those with lower amplitude. In the case where the interferogram is only affected by a low amplitude noise contribution, the Kasai algorithm thus improves the signal-to-noise ratio. In

Doppler mode, the delay line is adjusted such that the carrier frequency is zero, and the electro-optical modulator is driven by a saw-tooth synchronized to the delay line scanning thereby generating a carrier frequency of 3.2 MHz [5]. In this mode, the lateral displacement is also controlled by the FPGA. In the analog mode, the delay line generates the carrier frequency of 3.2 MHz by proper adjustment of the pivoting mirror offset. In addition, the lateral scan is then generated by an external saw-tooth generator.

To suppress noise induced by motion of probe or sample, the hand-held probe was mounted on a supporting arm for the in vivo skin measurements presented below. Furthermore a link between probe and skin was mounted to provide an angle of 74 degrees between surface and optical beam and provide stability. In general, blood flow was then more pronounced than when measuring with a beam perpendicular to the skin. This means that there is a tendency that blood vessels run parallel to the skin surface.

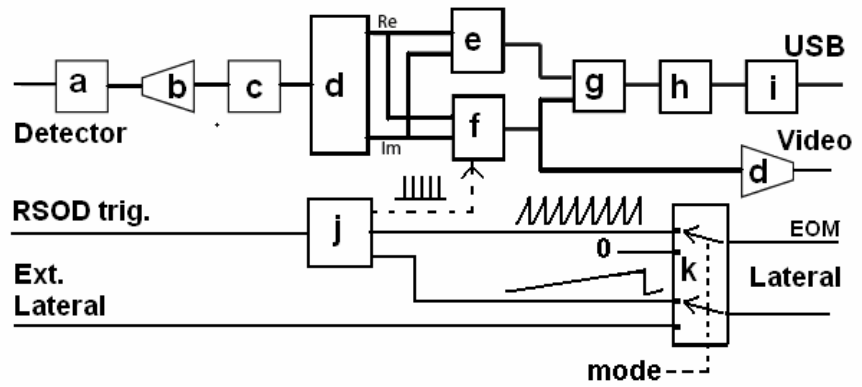

Figure 2. Algorithm for calculation of envelope and Doppler shift. a) Amplifier and analog band-pass filter. b) Analog-to-digital converter, 12 bit, 120 MS/s. c) Decimation by 8 low-pass filter. d) Conversion from real to complex analytic signal. e) Argument calculation and averaging using the Kasai autocorrelation. f) Magnitude and averaging of complex signal. g) Concatenation of envelope and phase for each pixel. h) buffer. i) USB2.0 interface adapter. j) line and frame timing. k) Switch selecting operational mode. Lateral displacement is either controlled by the FPGA or an external ramp generator.

3. SYSTEM CHARACTERISATION AND PRELIMINARY TESTS

To test the systems ability of detecting velocities, we did measurements on a flow phantom with known flow velocity. A picture of the setup used for the measurements is shown in Figure 7a. The stationary solid phantom was a mixture of epoxy resin, hardener, ink, and TiO_2-particles aiming for optical properties close to biological tissue. In a depth of 150 μm in the stationary phantom, a small flow channel with a diameter of 400 μm had been drilled as shown in Figure 3b. For all measurements, we used an intralipid 2%-solution for the flow phantom, and an angle of 80.2° between the flow channel and the optical beam. An example is shown in Figure 3c, with the flow profile in Figure 3d through the centre of the flow channel. To extract the peak or maximum velocity in the flow channel, a 2nd order polynomial fit is used. In Figure 4, the peak velocity determined by the Doppler OCT system is plotted as a function of the pump peak velocity. As expected for a laminar flow, the curve shows a linear relation between the pump flow velocity and the velocity measured with the Doppler OCT system. A minimum detectable average flow velocity of ~0.3 mm/s was estimated.

In order to prepare for the clinical measurements on patients we performed measurements on normal skin to optimize the system. In Figure 5 an example of a normal skin ODT image acquired on the palm of a hand is shown illustrating that we are able to measure flow velocities typically found in skin. During these tests, an interesting observation was made. By following a blood vessel over a few minutes, the flow showed a periodic variation with a change between maximum and almost zero activity. The period of the variation was on a scale of minutes or less and was reproducible. The blood

vessels chosen for these measurements were relatively large with a size of about 200-300 µm, and we therefore believe that the effect is real and not due to small changes in probe position or angle. The observation is in agreement with previous findings recording oxygen tension in the human forearm [10]. The periodic changes is a complication to monitoring blood flow changes because it can not necessarily be distinguished whether a change in blood flow is caused directly by the PDT treatment, or just reflects a natural fluctuation. Only by averaging blood flow activity for a time much longer than the period of the natural cycle one can compensate for this effect. This requires measurement durations of at least a few minutes. Assuming a constant blood flow period, an alternative could be to measure in the same phase of the period. This approach would allow comparing blood flow acquired in shorter duration times. However, the stability of the periodic blood flow pattern should be investigated beforehand.

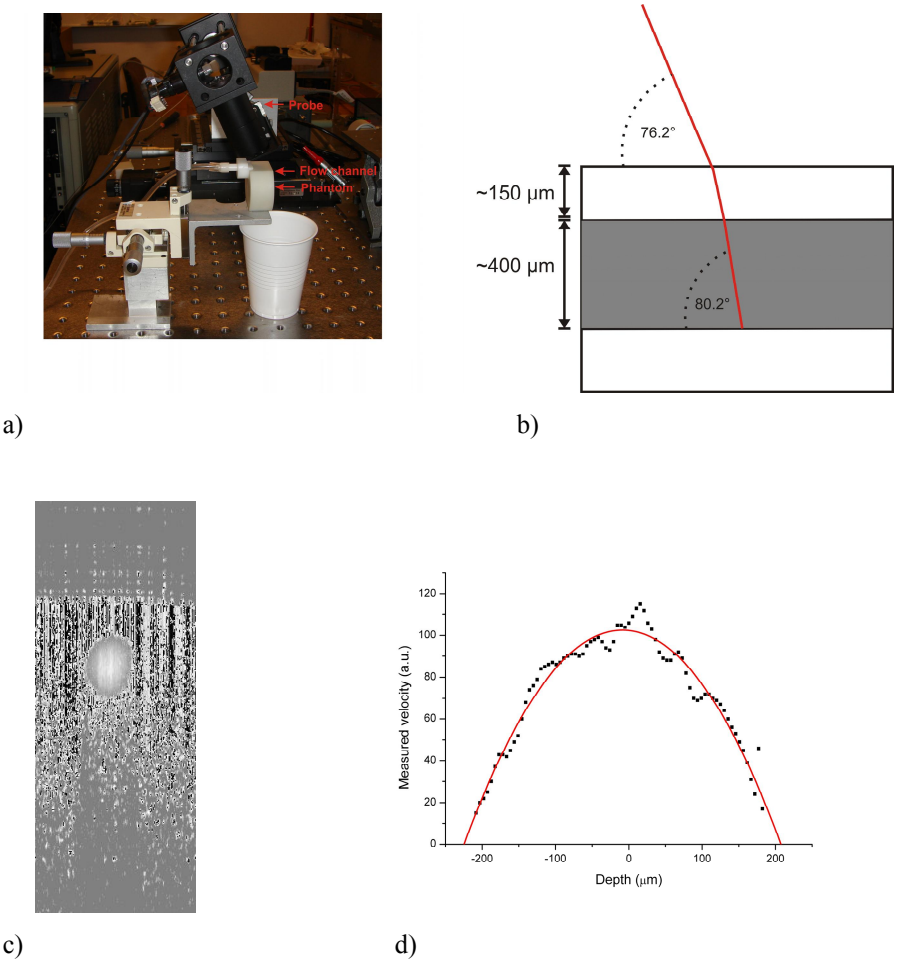

Figure 3. Setup for phantom measurements. a) photo of the setup b) sketch of the setup showing relevant angles c) ODT image of the phantom with a flow velocity of 4 mm/s d) corresponding plot of A-scan from the image and a parabolic fit.

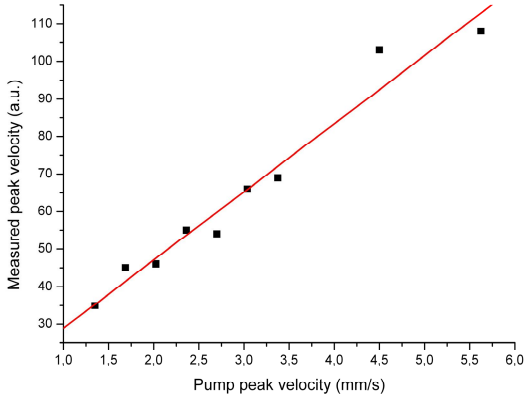

Figure 4. Calibration curve obtained from the phantom measurements. As expected a linear relation between pump velocity and measured phase shift is demonstrated.

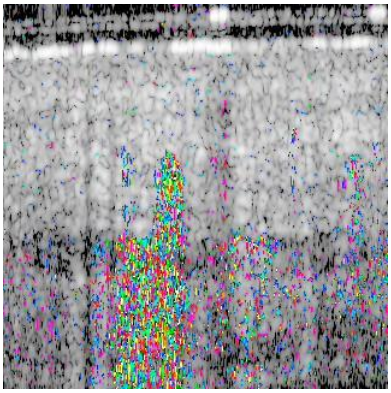

Figure 5. ODT image acquired on the palm of a hand showing the presence of a blood vessel in dermis (width: 1.3 mm, height: 1.5 mm)

4. MEASUREMENTS ON SKIN TUMORS DURING PHOTODYNAMIC THERAPY

Following the tests described above, we moved on to clinical measurements on patients with skin tumors. We aimed for measuring the blood flow activity before, during and after photodynamic therapy. First, the sensitizer, in this case 20% ALA cream, was applied to the patients. A few hours are then needed for absorption and distribution within the tumor. Then, the tumor area is illuminated for about 15 minutes with red light to excite the sensitizer and complete tumor destruction. For all images, 8 A-scans were acquired at each lateral location to calculate the phase shift resulting in an acquisition time of ~0.7 s. for a 1.3 mm wide image. Using fewer A-scans for calculating the phase shift results in faster imaging acquisition but unfortunately also in more pronounced noise.

We expected an increased blood flow near a tumor compared to normal skin because a tumor is characterized by having a high supply of sugar through the blood. However, this was not confirmed by our measurements, we observed only very limited blood flow near tumors just like in most normal skin. The observations for normal skin is in agreement with a study using laser Doppler flowmetry reporting an average dermal blood concentration of about 1% or less depending on the site of the skin [11].

Due to the limited blood flow around skin tumors, it was very critical to measure at the same position on the skin to compare blood flow at different times. This requirement would have been more relaxed if blood flow around a tumor was more pronounced and homogeneous. Measuring at the same position proved impossible and therefore we are not able to conclude whether blood flow changes during PDT treatment. Furthermore, variations due to the pressure of the probe on the skin were observed. Therefore, it is important to apply the same pressure every time, and especially to avoid a high pressure that limits the flow. In Figure 6, a single frame acquired on scar tissue after radiation therapy of a tumor is shown for illustration showing a superficial blood vessel. The frame is part of a movie showing a pulsative nature of the blood flow. In conclusion, we are able to detect blood flow but investigating blood flow changes during PDT of human skin tumors is not possible with the setup presently used due to practical issues.

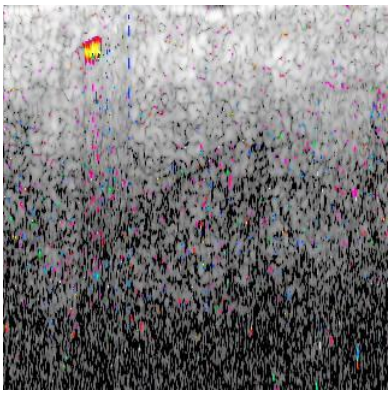

Figure 6. Measurements performed on the stomach of a 62 year old woman with scar tissue due to radiation therapy of skin cancer. The colored spot corresponds to a superficial blood vessel (width: 1.3 mm, height: 1.5 mm).

5. SUMMARY AND OUTLOOK

As mentioned above, the results of these measurements are extremely sensitive to motion, position and pressure on the skin. When the goal is to measure changes in vascularization, it is critical to measure at the same position within the width of the B-scan. Since the width corresponds to the spot size of the beam, we must be able to position the probe with an accuracy of less than ~ 30 μm. In practice, this is very difficult. Therefore, it is necessary to have a setup with a probe that is not moved in between the measurements. This can be accomplished by using an interstitial ODT implementation with a needle placed in or around the tumor measuring continuously during PDT as demonstrated by Li et al [3]. However, a needle implementation of ODT can also affect the blood flow which should be taken into account. Minimization of noise induced by motion of the probe is important, and a faster data acquisition is therefore preferred. This can be accomplished with Fourier domain systems [12]. Using a state-of-the-art Fourier domain ODT system would also allow acquiring three dimensional data very fast. Because a larger surface area is then covered, the position of the probe from time to time is less critical than when using only a single B-scan. Natural fluctuations should also be considered and requires for example averaging over time. Finally, we only detected the presence of blood flow and did not measure the absolute value of the velocity. It is also relevant to measure absolute velocities which have been demonstrated without prior knowledge of the angle between the optical beam and the flow direction in the blood vessel [13]. With these improvements of the setup, we believe that future measurements can provide knowledge of blood flow changes during a PDT treatment.

REFERENCES

1. T. J. Dougherty, C. J. Gomer, B. W. Henderson, G. Jori, D. Kessel, M. Korbelik, J. Moan, and Q. Peng, *"Photodynamic therapy*", J. Natl. Cancer Inst., **90**(12), 889-905 (1998)

2. S. Pålsson et al, "*Kinetics of the superficial perfusion and temperature in connection with photodynamic therapy of basal cell carcinomas using esterified and non-esterified 5-aminolaevulinic acid"*, Br. J. of Derm., **148**, 1179-1188 (2003).

3. H. Li et al, *"Feasibility of Interstitial Doppler Optical Coherence Tomography for In Vivo Detection of microvascular Changes During Photodynamic Therapy",* Lasers in Surg. and Med., **38**, 754-761 (2006)

4. G. J. Tearney, B. E. Bouma, and J. G. Fujimoto, "*High-speed phase- and group-delay scanning with a grating-based phase control delay line*", Opt. Lett., **22**, 1811-1813 (1997)

5. J. F. de Boer, C. E. Saxer, and J. S. Nelson, "*Stable carrier generation and phase-resolved digital data processing in optical coherence tomography*", Appl. Opt., **40**, 5787-5790 (2001)

6. H. E. Larsen, R. T. Nilsson, L. Thrane, F. Pedersen, T. M. Jørgensen, P. E. Andersen, "*Optical Doppler tomography based on a field programmable gate array*", Biomed. Sign. Proc. and Contr., **3**, 102-106 (2008)

7. Y. Zhao, Z. Chen, C. Saxer, S. Xiang, J. F. de Boer, and J. S. Nelson, *"Phase-resolved optical coherence tomography and optical Doppler tomography for imaging blood flow in human skin with fast scanning speed and high velocity sensitivity*", Opt. Lett., **25**, 114-116 (2000)

8. V. X. D. Yang, M. L. Gordon, A. Mok, Y. Zhao, Z. Chen, R. S. C. Cobbold, B. C. Wilson, and I. A. Vitkin, "*Improved phase-resolved optical Doppler tomography using the Kasai velocity estimator and histogram segmentation*" Opt. Comm., **208**, 209-214 (2002)

9. C. Kasai, K. Namekawa, A. Koyano, and R. Omoto, "*Real-time two-dimensional blood-flow imaging using an auto-correlation technique*" IEEE Trans. on Sonics and Ultrasonics, **32**, 458-464 (1985)

10. N. T. S. Evans, P. F. D. Naylor, B. McA. Sayers, "*The spatial correlation of fluctuations of the blood flow in forearm skin*", Br. J. of Derm., **96**(6), 609-614 (1977)

11. I. Fredriksson, M. Larsson, T. Strömberg, "*Optical microcirculatory skin model: assessed by Monte Carlo simulations paired with in vivo laser Doppler flowmetry*", J. of Biomed. Opt., **13**(1), 014015 (2008)

12. A. Mariampillai, B. A. Standish, N. R. Munce et al, *"Doppler optical cardiogram gated 2D color flow imaging at 1000 fps and 4D in vivo visualization of embryonic heart at 45 fps on a swept source OCT system"*, Opt. Express, 15, 1627-1638 (2007)

13. L. Wu, "*Simultaneous measurement of flow velocity and Doppler angle by the use of Doppler optical coherence tomography",* Opt. Lasers Eng., **42**, 303-313 (2004)